β-Amyloid 25 to 35 Is Intercalated in Anionic and Zwitterionic Lipid Membranes to Different Extents

Silvia Dante,*[†] Thomas Hauss,*[†] and Norbert A. Dencher*

*Physical Biochemistry, Darmstadt University of Technology, D-64287 Darmstadt, Germany; and [†]BENSC, Hahn-Meitner Institut, D-14109 Berlin, Germany

ABSTRACT Neuronal plasma membranes are thought to be the primary target of the neurotoxic β-amyloid peptides (Aβ) in the pathogenesis of the Alzheimer's disease. Histologically, Aβ peptides are observed as extracellular macroscopic senile plaques, and most biophysical techniques have indicated the presence of Aβ close to the lipid headgroup region but not in the core of the membrane bilayers. The focus of this study is an investigation of the interaction between Aβ and lipid bilayers from a structural point of view. Neutron diffraction with the use of selectively deuterated amino acids has allowed us to determine unambiguously the position of the neurotoxic fragment Aβ (25–35) in the membrane. Two populations of the peptide are detected, one in the aqueous vicinity of the membrane surface and the second inside the hydrophobic core of the lipid membrane. The location of the C terminus was studied in two different lipid compositions and was found to be dependent on the surface charge of the membrane. The localization of β-amyloid peptides in cell membranes will offer new insights on their mechanism in the neurodegenerative process associated with Alzheimer's disease and might provide clues for therapeutic developments.

INTRODUCTION

Although their mechanism of action in the neurodegenerative process has not been yet established, the β-amyloid peptides play an important role in the pathogenesis of Alzheimer's disease (Beyreuther and Masters, 1997). The senile plaques, typical histological lesions in the brain tissues of Alzheimer's disease patients, are extracellular deposits of Aβ peptides; they contain mainly fibrils of Aβ with 39 to 43 amino acid residues, intermixed with shorter fragments of the peptide in amorphous form (Selkoe, 1999). Besides neuritic plaques, Alzheimer's disease is also characterized by intraneuronal tangles of polymerized τ protein (Mandelkow and Mandelkow, 1998). These two lesions can develop independently of each other and can appear in different regions of the brain of Alzheimer patients, but there is evidence that Aβ may trigger the cytological response that leads to the formation of neurofibrillary tangles (Selkoe, 1999). Nevertheless, it is not clear whether it is the extracellular Aβ accumulation that initiates the neurotoxic response or if it is the monomeric (or oligomeric) form of Aβ that is capable of diffusing and accumulating at specific target sites, thereby activating the cascade of pathogenic changes in brain tissues.

Aβ is a 39 to 43 amino acid residue peptide produced by proteolytic cleavage of the amyloid precursor protein by γ-secretase (Haass and De Strooper, 1999). Aβ spontaneously aggregates in amyloid fibrils, whose toxicity to cultured cortical cells is well known (Busciglio et al., 1995; Mattson et al., 1992; Pike et al., 1993). Much of the biological activity of the full-length peptide is possessed by the 11 residues fragment Aβ (25–35). In fact, this fragment has been proved to have a cytotoxic effect on human cerebral cortical cell cultures (Mattson et al., 1992) and to modulate membrane lipid peroxidation (Walter et al., 1997). Its three-dimensional structure in a membrane-mimicking environment has been solved by NMR study (Kohno et al., 1996), revealing an α-helix structure in the C-terminal region, embedded in detergent micelles. This model would fit with the hydrophobicity of the seven amino acid residues in the C terminus, most likely to be embedded in the membrane, whereas the four residues of the N terminus, including a positively charged lysine, would be in the vicinity of the hydrophilic environment.

Several studies indicate that Aβ neurotoxicity may be mediated, at least in part, by direct interactions between the peptide and the membrane lipids. In particular Aβ (1–40) forms cation-selective channels across acidic phospholipid bilayer membranes, and it was suggested that these channels disrupt ion homeostasis and hence cause toxicity (Arispe et al., 1993; Mirzabekov et al., 1994). Membrane disruption by Aβ peptides mediated through binding to phospholipids or protein membranes has also been reported (McLaurin and Chakrabartty, 1996).

A prerequisite for any understanding of the interaction of the peptide with the membrane is knowledge of its exact location at the membrane. At present, the published data are highly controversial (Mason et al., 1999; Shao et al., 1999; Terzi et al., 1994, 1997), and most results have been obtained by the application of indirect methods and/or inappropriate target systems such as lipid monolayers or detergent micelles. Besides the overwhelming quantity of papers considering the extracellular location of Aβ in the senile plaques, some studies suggest that the Aβ peptides bind

electrostatically only to the polar headgroups, i.e., do not become embedded within the hydrophobic interior. On the other hand, the only structural localization by x-ray diffraction indicates that the fragment Aβ (25–35) inserts, at physiological pH, into the hydrophobic core of net-uncharged lipid membranes (Mason et al., 1996).

We investigated the interaction of Aβ (25–35) with oriented lipid bilayer samples by neutron diffraction, and the interaction and depth of penetration of the C terminus in the bilayer core were determined. Neutron diffraction experiments are indeed a sensitive and direct method for delineating the structure of the bilayer profile. In the study of biological samples, the advantage of neutron diffraction is based on the large difference in the scattering length of hydrogen ($b_H = -0.37 \times 10^{-14}$ m) and deuterium ($b_D = 0.67 \times 10^{-14}$ m). Using the isomorphous replacement technique it is therefore possible to locate, with high sensitivity and without perturbing the system, a selectively deuterated part of a molecule in a structure even at lower spatial resolution. This approach is often applied; it was used for instance to analyze the location of retinal in bacteriorhodopsin (Hauss et al., 1990) and, more recently, to study the interaction of short peptides, like substance P, with phospholipid membranes (Bradshaw et al., 1998). In the present study the penultimate amino acid in the C-terminal region of Aβ (25–35), a leucine containing 10 hydrogens, was selectively deuterated. Diffraction patterns obtained from lipid samples containing the deuterated and the protonated species of Aβ (25–35), respectively, were compared. A mixture of 92:8 mol/mol of 1-palmitoyl-2-oleoyl-phosphatidylcholine (POPC) and 1-palmitoyl-2-oleoyl-phosphatidylserine (POPS) was used to mimic, as closely as possible, the composition and the negative charge state of neuritic cell membranes without increasing the complexity of the system too much. To gain information about the effect of anionic lipids on the peptide/membrane interaction, a system in which the lipid matrix consisted of neutral lipids only (i.e., POPC) was also investigated.

MATERIALS AND METHODS

Sample preparation

Aβ (25–35) peptide (GSNKGAIIGLM) was synthesized and purified to 95% by WITA GmbH (Teltow, Germany). Two batches of the peptide were prepared, one protonated and one containing a deuterated leucine (10 deuterons) at position 34. To avoid preaggregation and to maintain the peptide in its monomeric form, a pretreatment with trifluoroacetic acid (TFA) (Jao et al., 1997) was applied. The peptide-TFA solution was dried in a quartz tube under a stream of nitrogen and put under vacuum ($p < 1$ mbar) for 12 h to remove all traces of TFA.

POPC and the net negatively charged lipid POPS were purchased from Avanti Polar Lipid (Alabaster, AL). Chloroform solutions both of POPC or of a mixture of POPC/POPS (92:8 m/m) were prepared and added to the dried pretreated peptide. The samples contained 20 mg of lipids and 3 mol% peptide to have a sample with Aβ concentration as low as possible. This condition was chosen on the basis of our previous successful work on

the localization of deuterated retinals in bacteriorhodopsin (Hauss et al., 1990). In that case the difference in scattering length between the membranes with deuterated and protonated retinals, respectively, was in the range of 6% to 13%. We chose, therefore, a peptide to lipid ratio resulting in a difference of scattering length in the same range (i.e., 13.8% in 100% H_2O). Control samples, containing only the lipid mixtures, were also prepared. To check the reproducibility of the sample preparation, we produced a second independent sample with a POPC/POPS mixture and protonated peptide; this sample was scanned in a second measuring time at the membrane diffractometer.

Oriented samples were obtained by spraying the solutions, using an artist's airbrush, onto quartz slides (65 mm × 15 mm × 0.3 mm), covering only the central area of one side. Traces of the solvent were removed by placing the slides in a vacuum dessicator for 12 h ($p < 1$ mbar). Samples were then rehydrated for 24 h at room temperature in an atmosphere of 98% relative humidity, maintained with a saturated K_2SO_4 solution. Since the samples were rehydrated in this way, they contained pure water, with no salts, and it was not possible to measure the pH of the samples.

Neutron diffraction and data analysis

Neutron diffraction measurements were carried out on the membrane diffractometer V1 at the Berlin Neutron Scattering Center of the Hahn-Meitner-Institute (Berlin, Germany). The samples were placed vertically in a standard aluminum container in which the temperature was controlled ($T = 27.0 \pm 0.1°C$ for all samples) and humidity adjusted by aqueous saturated solutions of K_2SO_4 in Teflon water baths at the base of the chamber. A temperature gradient between sample and container can be excluded because no condensation was observed on the samples or inside the can after each experiment. Contrast variation was achieved by adjusting the atmosphere in the sample container to three different compositions of $D_2O:H_2O$ (i.e., 100:0, 50:50, and 0:100). After each change of the aqueous solution, the samples were let to equilibrate for 24 h.

Preliminary θ-2θ scans were performed to check the absence of nonlamellar reflections. Diffraction intensities were measured with rocking scans, rocking the sample around the expected Bragg position θ by $\theta \pm 2°$. The duration of each rocking scan varied from 20 min to 4 h depending on the intensity of the reflection. To control the equilibrium state of the samples, we performed the scans of the complete series of the Bragg peaks twice, checking the reproducibility in intensity and position of each reflex, which were found to be identical, within experimental error limits, for all measurements. Diffraction patterns of POPC and POPC/POPS bilayers of POPC and POPC/POPS bilayers containing 3% (mol) (D-Leu-34)-Aβ (25–35) and of POPC and POPC/POPS containing 3% (mol) (H-Leu-34)-Aβ (25–35) were measured (data not shown). The lamellar spacing d of each sample was calculated by least-square fitting of the observed 2θ values to the Bragg equation $n\lambda = 2d \times \sin\theta$, in which n is the diffraction order and λ is the selected neutron wavelength (4.53 Å). Integrated intensities were calculated with Gaussian fits to the experimental Bragg reflections; due to the intensity distribution of the primary neutron beam, a Gaussian is a very good approximation of the shape of a reflection. Intensities, corrected with absorption and Lorentz factors, were square-rooted to produce the structure factor amplitudes. We calculated the linear absorption coefficient μ for $\lambda = 4.53$ Å to $\mu = (5.55 - x \times 1.05)$ cm^{-1} (x is the mole ratio $H_2O:D_2O$) with the scattering cross-sections found in Sears (1992) according to the formula given in Franks and Lieb (1979). The largest absorption correction occurred in 100% H_2O for the first Bragg reflex and was 1.7%.

The data were placed on a "relative absolute" scale following a procedure described by Wiener and White (1991) using the known neutron scattering length of D and H to scale the differences between homologous samples in D_2O and H_2O atmosphere and between homologous deuterated and protonated samples. The number of water molecules, necessary to perform the scaling, was measured gravimetrically. The samples were repeatedly weighted in the wet and in the dry state, and from the weight difference the amount of water was determined with precision better than 5%. This procedure gave 16.2 ± 1.8

TABLE 1 Experimental structure factors of all the samples investigated, corrected, and scaled as described in the text

	$F(0)$	$F(1)$	$F(2)$	$F(3)$	$F(4)$	$F(5)$
			POPC/POPS			
100% D_2O		-31.2 ± 0.1	10.9 ± 0.5	2.17 ± 0.07	0	-6.15 ± 0.06
50% D_2O		-16.4 ± 0.2	1.64 ± 0.01	4.37 ± 0.08	0	-5.74 ± 0.05
0% D_2O	0.31 ± 0.02	-1.57 ± 0.01	-7.63 ± 0.05	4.37 ± 0.03	0	-4.37 ± 0.05
		POPC/POPS $+$ Aβ(25–35) protonated sample 1				
100% D_2O		-26.80 ± 0.3	10.2 ± 0.1	2.04 ± 0.02	0	-2.95 ± 0.04
50% D_2O		-14.72 ± 0.1	1.00 ± 0.03	3.36 ± 0.03	0	-2.54 ± 0.05
0% D_2O	0.36 ± 0.02	-2.65 ± 0.02	-8.78 ± 0.05	4.50 ± 0.03	0	-2.08 ± 0.04
		POPC/POPS $+$ Aβ(25–35) protonated sample 2				
100% D_2O		-25.56 ± 0.3	12.7 ± 0.1	2.01 ± 0.02	-1.05 ± 0.05	-3.90 ± 0.04
50% D_2O		-14.46 ± 0.1	1.64 ± 0.04	3.60 ± 0.03	-0.46 ± 0.05	-3.15 ± 0.04
0% D_2O	0.45 ± 0.03	-2.30 ± 0.02	-8.45 ± 0.04	5.05 ± 0.04	0	-2.50 ± 0.04
		POPC/POPS $+$ Aβ(25–35) deuterated				
100% D_2O		-29.96 ± 0.3	10.69 ± 0.01	2.12 ± 0.02	0	-3.25 ± 0.03
50% D_2O		-16.30 ± 0.2	1.34 ± 0.02	3.05 ± 0.02	0	-2.81 ± 0.03
0% D_2O	1.32 ± 0.06	-2.66 ± 0.06	-7.72 ± 0.01	3.78 ± 0.03	-1.20 ± 0.05	-2.37 ± 0.02
		POPC				
100% D_2O		-37.9 ± 0.4	18.8 ± 0.1	2.43 ± 0.08	-3.12 ± 0.18	-7.03 ± 0.5
50% D_2O		-24.46 ± 0.2	2.84 ± 0.01	6.44 ± 0.10	-2.68 ± 0.16	-5.91 ± 0.6
0% D_2O	1.37 ± 0.06	-4.34 ± 0.06	-12.83 ± 0.05	10.36 ± 0.07	-0.81 ± 0.05	-4.51 ± 0.5
		POPC $+$ Aβ(25–35) protonated				
100% D_2O		-42.31 ± 0.3	17.9 ± 0.1	2.84 ± 0.10	-4.13 ± 0.3	-7.2 ± 0.5
50% D_2O		-25.09 ± 0.2	2.71 ± 0.08	6.46 ± 0.17	-3.94 ± 0.4	-5.4 ± 0.6
0% D_2O	1.60 ± 0.06	-4.34 ± 0.04	-13.4 ± 0.1	9.97 ± 0.10	-2.68 ± 0.3	-4.30 ± 0.35
		POPC $+$ Aβ(25–35) deuterated				
100% D_2O		-50.05 ± 0.5	22.0 ± 0.2	4.36 ± 0.4	0	-7.03 ± 0.4
50% D_2O		-27.74 ± 0.3	3.26 ± 0.03	7.26 ± 0.19	0	-6.88 ± 0.4
0% D_2O	1.68 ± 0.08	-3.89 ± 0.04	-15.6 ± 0.1	9.97 ± 0.20	0	-6.20 ± 0.7

The reported errors are derived from the counting statistics and baseline variation. $F(0)$ values are derived from the lipid membrane composition and the water content of each sample (see text) and are in units of 10^{-14} m.

and 10.0 ± 1.5 water molecules per lipid for the POPC/POPS and POPC mixtures, respectively. The error in the determination of the number of water molecules results in an error in the average scattering length density per unit length (Wiener and White, 1991).

The relative absolute density profile $\rho(z)$ is given by

$$\rho(z) = \frac{2}{d} \sum_{h=0}^{n} F(h) \cos\left(\frac{2\pi hz}{d}\right) \quad (1)$$

in which F is in units of scattering length and $\rho_0(z) = \frac{2}{d} F_0$ is the average scattering length per unity length of the bilayer, $F(h)$ are the scaled structure factors, and the sum describes the distribution in scattering lengths across the bilayer.

To estimate the significance of any feature in the scattering length density profiles, knowledge of the error limits in the profiles is necessary. The error in the scattering length density profiles corresponding to the desired confidence limit is given by:

$$\Delta\rho(z) = t\{\mathrm{var}(\rho(z))\}^{1/2} \quad (2)$$

in which t is the Student's t factor and $\mathrm{var}(\rho(z))$ the variance of $\rho(z)$. Because the structure factors are independent of each other, Eq. 2 reads:

$$\Delta\rho(z) = \frac{2t}{d}\left[\sum_{h=0}^{n}(\Delta F(h))^2 \cos^2\left(\frac{2\pi hz}{d}\right)\right]^{1/2} \quad (3)$$

The error ΔF was first determined with the counting statistics and the variation of the baseline for each reflection and is given in Table 1. In an ideal experiment the differences of corresponding structure factors between samples with protonated and deuterated peptide in various $D_2O:H_2O$ ratios

are identical within the statistical error limit. In a real experiment systematical errors may contribute to the measured data points. In our experiment a slight difference in humidity introduce such an error. An estimate of the error comes from the comparison of any difference between corresponding data points and is used in the further analysis. The confidence limit used in this paper was 95% ($t = 1.96$).

The phase assignment was obtained with the isomorphous replacement method, using the $D_2O:H_2O$ exchange, where the structure factors are linear function of the mole fraction $D_2O:H_2O$ (Franks and Lieb, 1979). Structure factors at three different isotopic water vapor compositions were measured for each sample. For any further data evaluation, i.e., for the localization of the label, only the structure factors obtained at 0% D_2O were used. It is not appropriate to use the structure factors at 100% or 50% D_2O to determine the label position via the Fourier difference method. At these contrasts the large coherent scattering of the water layer covers that of the membrane. The difference in coherent scattering length due to the labeled Aβ is reduced to 1.3% only compared with 13.8% in 100% H_2O and becomes barely detectable. The position of the deuterated amino acid was determined by the differences of the densities between samples with Aβ containing deuterated and protonated leucine on a relative absolute scale. The distribution of the label was fitted in reciprocal space to the position and amplitude of a Gaussian function using the measured structure factors up to the fifth order.

RESULTS AND DISCUSSION

Diffractograms showed up to five orders for each measured sample (data not shown). A mosaicity inferior to 0.5° was a

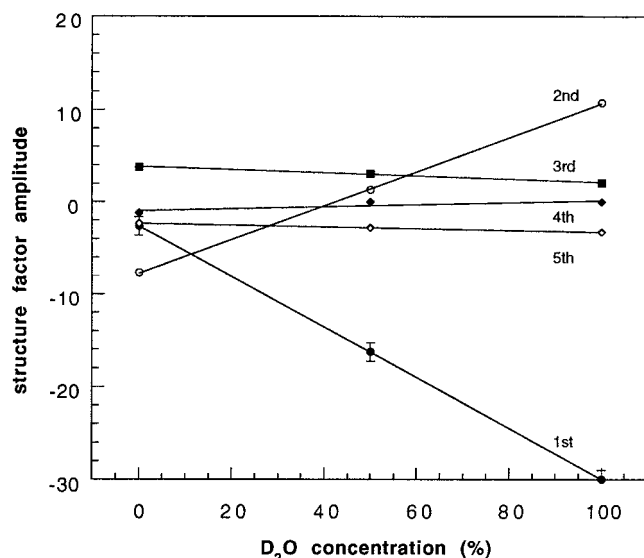FIGURE 1 Example of the structure factors and their phase assignment using H₂O/D₂O exchange, in this instance POPC/POPS multilayers containing deuterated Aβ (25–35). The errors are estimated as described in the text and where not shown are smaller than the symbols.

FIGURE 2 (*A*) Scattering length density profiles times lipid area ($\rho*z) \times S = \rho(z)$) in the direction normal to the membrane plane of the two samples containing deuterated (*solid*) and protonated (*dashed*) Aβ (25–35) in the case of an anionic POPC/POPS membrane. The profile of a pure lipid sample (*dotted*) is shown as a reference. (*B*) Difference scattering length density profile of the sample with protonated and deuterated Aβ (25–35) (*solid line*) and its fit to two Gaussian distributions (*dotted line*) truncated to the fifth Fourier term. Two distinct locations of the deuterated label occur, one of them is situated in the interior of the lipid bilayer, the second in the lipid/water interface. A model of the peptide is sketched to scale (*top*) with the leucine residue in two possible locations, according to our findings. The deuterons of the labeled leucine are colored gray. The peptide conformation is taken from Kohno et al., 1999. The sketch is only to guide the eye, because we have no information about the orientation of the peptide at present. However, with the presence of a positively charged lysine, an orientation with the N terminus in the vicinity of the negatively charged membrane surface can be inferred.

proof of the excellent quality of the samples. Significant relative intensity changes could be observed either between the pure lipid and the peptide containing samples and between the lipid samples containing the protonated and deuterated Aβ (25–35) peptide. Table 1 summarizes the structure factors experimentally determined, corrected, and scaled as described in Materials and Methods. F (0) values, calculated at 0% D₂O, are listed as well. Fig. 1 shows an example of the phase assignment of the structure factors using the D₂O/H₂O exchange. Here the assumption is made that the water layer can be modeled as a Gaussian centered at the unit cell boundaries; this defines the phases of the associated structure factors F_w as − + − + − for the first five orders. In Fig. 1 the functions $F = xF_w + F_M$, with F_M as structure factors of the membrane, are plotted as a function of the molar D₂O:H₂O ratio x. The structure factors in Table 1 are phased accordingly. The largest values of the difference structure factors for homologous samples are obtained for F_1 and F_2 in 100% D₂O. These structure factors are indeed the most sensitive to the difference in water content of the various samples, which is quite difficult to control at the high humidity levels. On the other hand, high humidity is desirable to stay as close as possible to physiological conditions.

POPC/POPS multilayers

The calculated d spacings at 98% relative humidity were 56.7 ± 0.4 Å, 56.9 ± 0.4 Å, and 57.0 ± 0.4 Å for the POPC/POPS, the POPC/POPS with protonated, and the POPC/POPS with deuterated Aβ (25–35), respectively. Fig.
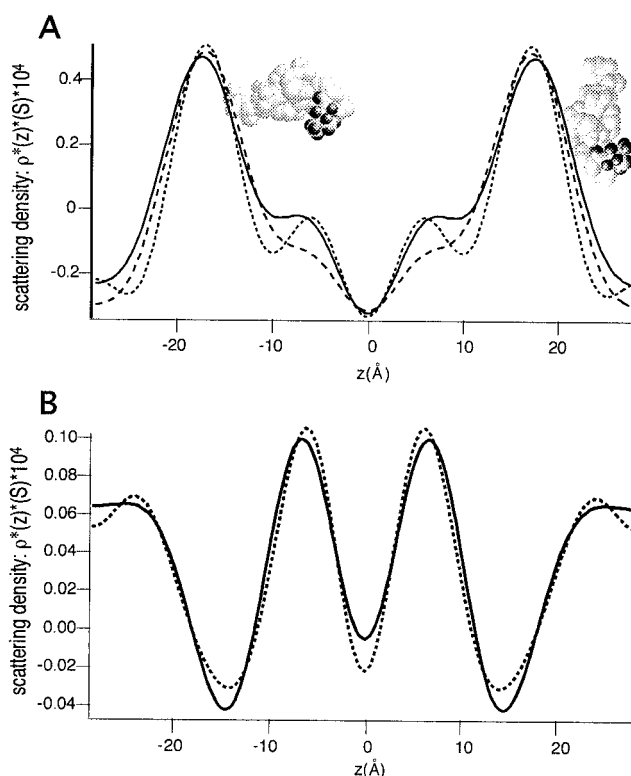
2 *A* exhibits the scattering length density profiles along the normal to the membrane plane obtained via Fourier synthesis from the structure factors at 0% D₂O as described in Materials and Methods. The reported patterns represent the elementary cell of the oriented samples, i.e., one lipid bilayer with its hydration shell; the center of the elementary cell is the middle of the bilayer profiles, occupied by the terminal methylene groups of the phospholipids. The water layers are centered at the two edges of the diagram at $z = -28.5$ Å and $z = 28.5$ Å. All the profiles were calculated using structure factors representing 0% D₂O as discussed in Materials and Methods. The two main peaks in the profiles (at −16.5 Å and 16.5 Å) represent the polar lipid headgroups, near the glycerol backbone, which contain fewer

TABLE 2 Results of fitting deuterium label distributions of Aβ (25–35) in bilayers of POPC/POPS and of POPC using Gaussian functions defined as $\rho(z) = A/\sqrt{2\pi}\sigma \exp(-(z - z_0)^2/2\sigma^2)$ for each label position

Membrane	σ(Å)	Parameter		Distribution
POPC/POPS	2.85	A (m)	$(1.02 \pm 0.1)\,10^{-14}$	54.0%
		z_0 (Å)	5.92 ± 0.16	
	2.85	A (m)	$(0.86 \pm 0.15)\,10^{-14}$	46.0%
		z_0 (Å)	24 ± 1	
POPC	2.85	A (m)	$(1.97 \pm 0.2)\,10^{-14}$	86.2%
		z_0 (Å)	14.3 ± 0.2	
	2.85	A (m)	$(0.31 \pm 0.09)\,10^{-14}$	13.8%
		z_0 (Å)	27.0 ± 0.2	

hydrogen atoms than the hydrocarbon region and have therefore a higher scattering length density. The unsaturated bond in the hydrocarbon chains of POPC and POPS is responsible for the secondary maximum at $|z| = 5.8$ Å in the scattering length density profile of the pure lipid sample (Büldt et al., 1979). The fact that the d spacings and the distances between the glycerol backbones do not vary between samples with and without peptide suggests that the peptide does not induce changes in the distance between membrane layers, in accordance with Mason et al. (1996).

The information about the location of the peptide comes from the difference of the profiles of the two samples containing labeled (Fig. 2 *A*, solid) and unlabeled (Fig. 2 *A*, dashed) Aβ. The difference of these two density maps gives in fact the deuterium distribution in the lipid bilayers containing (D-Leu-34)-Aβ (25–35). This distribution for anionic bilayers is shown in Fig. 2 *B* (solid line), and it suggests two separate locations for the label. We emphasize that this difference is in a "relative absolute scale," as explained in the experimental sections. To determine the deuterium distribution in the two label positions, a model fitting approach with two Gaussians (and their mirror images in the centrosymmetric unit cell) was considered. To perform this fitting procedure six parameters (i.e., amplitude, position, and width for each Gaussian) are necessary. Because our measurements are limited to five diffraction orders, we decided to use the experimental resolution as a fixed value for the width of the Gauss functions and to perform the fit with amplitudes and positions as free parameters. The fit results are reported in Table 2 and compared with the difference density in Fig. 2 *B*. The striking information is contained in the 54.0% of the deuterium located inside the membrane core at $|z| = 5.9$ Å, a position close to the double bond of the hydrophobic chains of the lipids. This is in qualitative agreement with the findings described by Mason et al. (1996). In that interesting paper based on x-ray diffraction, the authors put forward that Aβ (25–35) has lipophilic tendency. Our results support and extend the previous notion of the Aβ (25–35) being intercalated in the hydrocarbon core of a lipid bilayer by demonstrating unambiguously that the C-terminal part is located

near the center of the membrane. The paper by Mason et al. (1996) was hampered by the fact that no specific labeling was applied, i.e., samples with and without peptide were studied; this led to an overall location of the peptide relative to the membrane. Our results refine this finding and allow the conclusion that the C terminus has deeply penetrated into the bilayer. Moreover, in the study by Mason et al. (1996), the poor sensitivity of the method forced the authors to use an extremely high peptide/lipid ratio, i.e., 1:5 peptide/lipid mass, as compared with 1:24 in the present study. The use of unphysiological net uncharged lipid headgroups may also have been a limitation, because the electrostatic force between the negatively charged neuronal membranes and the net positively charged Aβ plays a role in their interaction, as shown by our results in the next section. Finally, the electron density profiles are reported in a relative arbitrary scale, which may be misleading, especially when differences are taken into account.

According to Fig. 2 *B*, a considerable amount of deuterium (46.0%) of the Aβ is in the aqueous medium. It is possible that a population of the peptide forms aggregates, which are not able to penetrate into the bilayers. This is in agreement with a previous study by Mason et al. (1999), where aggregates of Aβ (1–40) were located at the hydrophilic membrane region. On the other hand, it is also plausible that the peptides outside the membrane preserve the monomeric state, but the solubility threshold into the lipid phase has been reached. With the current data, it is not possible to discriminate between these two possibilities. Due to the small size of Aβ (25–35), the population of monomers versus aggregates cannot be detected by gel electrophoresis as in Mason et al. (1999). As a final remark, it can be observed that comparing the profiles of the two samples containing Aβ (25–35) with the pure lipid one (Fig. 2 *A*), a feature is clearly visible: the broadening of the region corresponding to the polar lipid headgroups. This fact raises the possibility of an overall disordering effect of peptide in the lipid headgroup region of the membrane structure.

The significance of the changes induced in the scattering length density profiles by the presence of the Aβ (25–35) peptide with respect to the error limits of $\rho(z)$ is illustrated in the left side of Fig. 3. The profiles of the membranes containing the labeled and the unlabeled peptide fragments are revealed together with their 95% confidence envelopes. It is clearly demonstrated that the peptide introduces changes in the membrane profiles well outside the error limits. The right side of Fig. 3 shows the two profiles obtained from two independent measurements of two independent samples in the presence of the protonated Aβ (25–35) peptide. These measurements demonstrate the reproducibility of the sample preparation and measurement, as the differences are well inside the confidence limit.

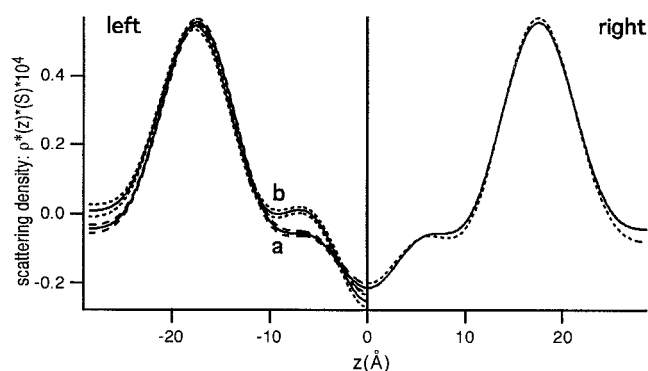At present, investigations using an Aβ fragment deuterated on the N-terminal side are being carried out. The

FIGURE 3   (*Left*) To demonstrate the quality of the data, the scattering length density profile of the POPC/POPS sample containing a protonated Aβ (25–35) is plotted (*solid lines*, *curve a*) together with the POPC/POPS sample containing deuterated Aβ (25–35) (*curve b*) on the left side and with a second POPC/POPS sample containing protonated Aβ (25–35) on the right side. On the left side the confidence limits are drawn (*dashed lines*). For simplicity only one-half of the unit cell is shown. The deuterons of the labeled peptide produced larger difference in the profiles than the confidence limits around $z = -28.5$ Å and $z = -5.9$ Å. The right side of the figure demonstrates the reproducibility of both sample preparation and measurements.

localization of this label will give the orientation of the Aβ (25–35) inside the bilayers.

POPC multilayers

The *d* repeats for the samples made of uncharged lipids were 53.9. ± 0.4 Å, 54.1 ± 0.4 Å, and 54.6 ± 0.5 Å for the POPC, the POPC with protonated, and the POPC with deuterated Aβ (25–35), respectively. The spacings for the net uncharged POPC were only approximately 3 Å smaller with respect to the spacings of the anionic membranes.

The scattering length density profiles in presence of the Aβ (25–35) are shown in Fig. 4 *A*, together with the POPC membrane profile. As in the case of the anionic membrane, the *d* spacing and the thickness of the membrane layers are unaffected by the presence of the peptide. The deuterium distribution in the lipid bilayers containing (D-Leu-34)-Aβ (25–35) is reported in Fig. 4 *B*. As in the case of POPC/POPS, two populations of the peptides are present, one inside and one outside the lipid bilayer. The results of the Gaussian model fit are presented in Table 2. With respect to POPC/POPS, a larger amount of the peptide (∼86.2%) is found inside the lipid membrane, but it does not intercalate as deeply in the is found at a position corresponding to the polar heads of the lipids, i.e., 14.3 ± 0.2 Å from the center of the membrane. This finding is in contrast to the study by Mason et al. (1996) where the same net-uncharged lipid membrane was used and the position of the peptide was determined close to the membrane center. The remaining 13.8% of the Aβ is localized in the aqueous medium, however, because this value is closed to the error limit it cannot be excluded that all the Aβ is localized at the lipid
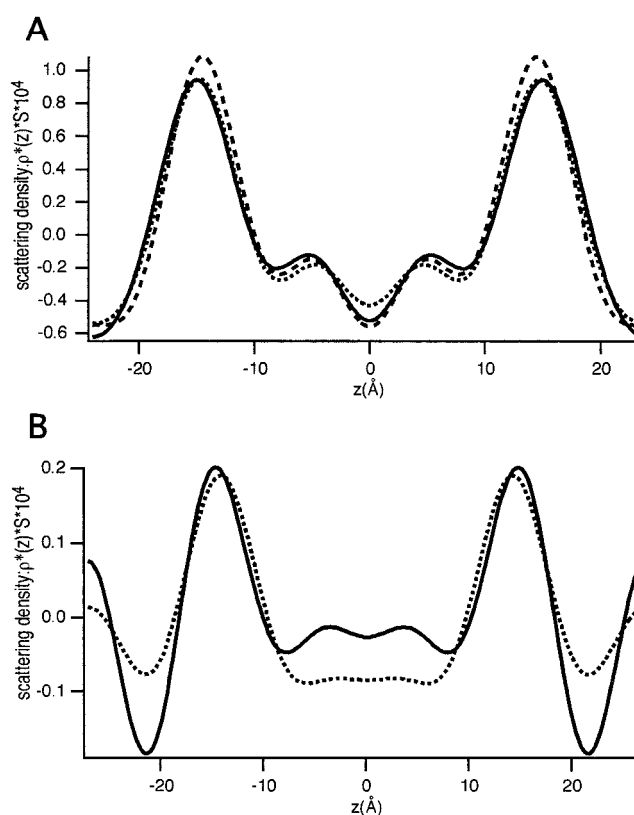

FIGURE 4   (*A*) Scattering length density times lipid area ($\rho*(z) \times S = \rho(z)$) along the direction normal to the membrane plane of the samples containing deuterated (*solid*) and protonated (*dashed*) Aβ (25–35) in the case of a POPC membrane. The profile of a pure POPC membrane is shown as dotted line. (*B*) Difference scattering length density profile, in the case of net uncharged POPC bilayers, between the sample with protonated and deuterated Aβ (25–35) (*solid line*) and its fit with two Gaussian distributions (*dotted line*), truncated to the fifth Fourier term. Two distinct locations of the deuterated label are observed, one of them is situated in a position corresponding to the lipid headgroups, the second in the water layer. Due to the restricted measuring time, the measurements were done only up to the fifth diffraction order, although in these samples higher orders were detectable. This led to Fourier truncation errors and noise in the Fourier density profiles.

headgroup region. As compared with the POPC/POPS membrane, a different behavior is observed in the lipid headgroup region, where no broadening between the membrane with and without peptide is observed.

Interaction of Aβ with charged and uncharged membranes

Our results are only in partial agreement with the study by Terzi et al. (1997) on lipid monolayers at the air/water interface. In that case, Aβ (1–40) was found to intercalate in the membrane in presence of anionic lipids, but only at packing density lower than that of a lipid bilayer. The study suggested that under physiological conditions, the peptide only bound electrostatic to the negatively

charged membrane. On the contrary, we observe a preferential intercalation of Aβ (25–35) with the hydrophilic lipid headgroups in absence of negatively charged lipids. As a matter of fact, it is not obvious that the peptide should interact the same way with the monolayer as with the bilayer system; differences can be expected especially when the insertion is deep inside the bilayer. Moreover, the systems investigated in the two studies differ both for the negatively charged lipid and for the length of the peptide used.

On the other hand, the similarities of our findings with the behavior of a peptide belonging to the tachykinin family, i.e., substance P, are remarkable. Aβ (25–35) and substance P are both 11-amino acid peptides with identical C-terminal region and with a positive charge in their sequence. Due to this resemblance, the Aβ (25–35) is often referred to as the tachykinin-like region of the Alzheimer's β-amyloid proteins, although it is not clear if it really shares any biological activities with tachykinins (El-Agnaf et al., 1998). In a previous study using neutron diffraction (Bradshaw et al., 1998), substance P was shown to intercalate in the membrane and moreover the intercalation was promoted by negatively charged lipids and hindered by zwitterionic ones. Furthermore, the penetration depth in the lipid core is nearly identical for the two peptides substance P and Aβ (25–35). This would indicate that the position of the C terminus in the membrane core is controlled by the membrane structure.

As demonstrated by our present study and recent experiments by others, lipid membranes are specific targets of Aβ peptides and the interaction Aβ/membrane might play a critical role in its neurotoxic mechanism. This is supported by the observation that Aβ forms cationic channels. The exact localization of the Aβ (25–35) C terminus in the hydrophobic core of phospholipid bilayers, as determined in the present study, can thus be exploited for the development of specific therapeutic drugs.

REFERENCES

Arispe, N., H. B. Pollard, and E. Rojas. 1993. Giant multilevel cation channels formed by Alzheimer disease amyloid β-protein [Aβ P-(1–40)] in bilayer membranes. *Proc. Natl. Acad. Sci. U. S. A.* 90:10573–10577.

Beyreuther, K., and C. L. Masters. 1997. Alzheimer's disease: the ins and outs of amyloid-β. *Nature.* 389:677–678.

Bradshaw, J. P., S. M. Davies, and T. Hauss. 1998. Interaction of substance P with phospholipid bilayers: a neutron diffraction study. *Biophys. J.* 75:889–895.

Büldt, G., H. U. Gally, J. Seelig, and G. Zaccai. 1979. Neutron diffraction studies on phosphatidylcholine model membranes: I. Head group conformation. *J. Mol. Biol.* 134:673–691.

Busciglio, J., A. Lorenzo, J. Yeh, and B. A. Yankner. 1995. β-amyloid fibrils induce tau phosphorylation and loss of microtubule binding. *Neuron.* 14:879–888.

El-Agnaf, O. M., G. B. Irvine, G. Fitzpatrick, W. K. Glass, and D. J. Guthrie. 1998. Comparative studies on peptides representing the so-called tachykinin- like region of the Alzheimer A β peptide [A β (25–35)]. *Biochem. J.* 336:419–427.

Franks, N. P., and W. R. Lieb. 1979. The structure of lipid bilayers and the effects of general anaesthetics: an x-ray and neutron diffraction study. *J. Mol. Biol.* 133:469–500.

Haass, C., and B. De Strooper. 1999. The presenilins in Alzheimer's disease-proteolysis holds the key. *Science.* 286:916–919.

Hauss, T., S. Grzesiek, H. Otto, J. Westerhausen, and M. P. Heyn. 1990. Transmembrane location of retinal in bacteriorhodopsin by neutron diffraction. *Biochemistry.* 29:4904–4913.

Jao, S. M. K., J. Talafous, R. Orlando, and M. G. Zagorski. 1997. Trifluoroacetic acid pretreatment reproducibly disaggregates the amyloid β-peptide. *Amyloid Int. J. Exp. Clin. Invest.* 4:240–244.

Kohno, T., K. Kobayashi, T. Maeda, K. Sato, and A. Takashima. 1996. Three-dimensional structures of the amyloid β peptide (25–35) in membrane-mimicking environment. *Biochemistry.* 35:16094–16104.

Mandelkow, E. M., and E. Mandelkow. 1998. Tau in Alzheimer's disease. *Trends Cell Biol.* 8:425–427.

Mason, R. P., J. D. Estermyer, J. F. Kelly, and P. E. Mason. 1996. Alzheimer's disease amyloid β peptide 25–35 is localized in the membrane hydrocarbon core: x-ray diffraction analysis. *Biochem. Biophys. Res. Commun.* 222:78–82.

Mason, R. P., R. F. Jacob, M. F. Walter, P. E. Mason, N. A. Avdulov, S. V. Chochina, U. Igbavboa, and W. G. Wood. 1999. Distribution and fluidizing action of soluble and aggregated amyloid β-peptide in rat synaptic plasma membranes. *J. Biol. Chem.* 274:18801–18807.

Mattson, M. P., B. Cheng, D. Davis, K. Bryant, I. Lieberburg, and R. E. Rydel. 1992. β-Amyloid peptides destabilize calcium homeostasis and render human cortical neurons vulnerable to excitotoxicity. *J. Neurosci.* 12:376–389.

McLaurin, J., and A. Chakrabartty. 1996. Membrane disruption by Alzheimer β-amyloid peptides mediated through specific binding to either phospholipids or gangliosides: implications for neurotoxicity. *J. Biol. Chem.* 271:26482–26489.

Mirzabekov, T., L. Meng-chin, Y. Wei-long, P. J. Marshall, M. Carman, K. Tomaselli, I. Lieberburg, and B. L. Kagan. 1994. Channel formation in planar lipid bilayers by a neurotoxic fragment of the β-Amyloid peptide. *Biochem. Biophys. Res. Commun.* 202:1142–1148.

Pike, C. J., D. Burdick, A. J. Walencewicz, C. G. Glabe, and C. W. Cotman. 1993. Neurodegeneration induced by β-amyloid peptides in vitro: the role of peptide assembly state. *J. Neurosci.* 13:1676–1687.

Sears, V. F. 1992. Neutron scattering lengths and cross sections. *Neutron News.* 3:26–37.

Selkoe, D. J. 1999. Translating cell biology into therapeutic advances in Alzheimer's disease. *Nature.* 399:A23–31.

Shao, H., S. Jao, K. Ma, and M. G. Zagorski. 1999. Solution structures of micelle-bound amyloid β-(1–40) and β-(1- 42) peptides of Alzheimer's disease. *J. Mol. Biol.* 285:755–773.

Terzi, E., G. Hölzemann, and J. Seelig. 1994. Alzheimer β-amyloid peptide 25–35: electrostatic interactions with phospholipid membranes. *Biochemistry.* 33:7434–7441.

Terzi, E., G. Hölzemann, and J. Seelig. 1997. Interaction of Alzheimer β-amyloid peptide(1–40) with lipid membranes. *Biochemistry.* 36:14845–14852.

Walter, M. F., P. E. Mason, and R. P. Mason. 1997. Alzheimer's disease amyloid β peptide 25–35 inhibits lipid peroxidation as a result of its membrane interactions. *Biochem. Biophys. Res. Commun.* 233:760–764.

Wiener, M. C., and S. H. White. 1991. Fluid bilayer structure determination by the combined use of x-ray and neutron diffraction: II. "Composition-space" refinement method. *Biophys. J.* 59:174–185.